

# Cis-Configured Aziridines Are New Pseudo-Irreversible Dual-Mode Inhibitors of *Candida albicans* Secreted Aspartic Protease 2

Björn Degel,<sup>[a]</sup> Peter Staib,<sup>[b, d]</sup> Sebastian Rohrer,<sup>[a, c]</sup> Josef Scheiber,<sup>[a]</sup> Erika Martina,<sup>[a]</sup> Christian Büchold,<sup>[a]</sup> Knut Baumann,<sup>[a, c]</sup> Joachim Morschhäuser,<sup>[b]</sup> and Tanja Schirmeister<sup>\*[a]</sup>

A series of cis-configured epoxides and aziridines containing hydrophobic moieties and amino acid esters were synthesized as new potential inhibitors of the secreted aspartic protease 2 (SAP2) of *Candida albicans*. Enzyme assays revealed the N-benzyl-3-phenyl-substituted aziridines **11** and **17** as the most potent inhibitors, with second-order inhibition rate constants ( $k_2$ ) between 56 000 and 121 000  $M^{-1} min^{-1}$ . The compounds were shown to be pseudo-irreversible dual-mode inhibitors: the intermediate esterified enzyme resulting from nucleophilic ring opening was hydrolyzed and yielded amino alcohols as transition-

state-mimetic reversible inhibitors. The results of docking studies with the ring-closed aziridine forms of the inhibitors suggest binding modes mainly dominated by hydrophobic interactions with the S1, S1', S2, and S2' subsites of the protease, and docking studies with the processed amino alcohol forms predict additional hydrogen bonds of the new hydroxy group to the active site Asp residues. *C. albicans* growth assays showed the compounds to decrease SAP2-dependent growth while not affecting SAP2-independent growth.

## Introduction

The yeast *Candida albicans* is a commensal on the mucosal surfaces in most healthy people. However, it can also cause serious infections, predominantly in immunocompromised individuals such as HIV patients, transplant recipients, or cancer patients undergoing chemotherapy.<sup>[1]</sup> These mycoses are difficult to treat, and the problem is accentuated by the emergence of fungal strains resistant to antifungal agents in current use.<sup>[2]</sup> In light of these developments, new antifungal agents with different mechanisms of action are needed. New drug targets are the secreted aspartic proteases (SAPs) of *C. albicans*, which are required for full virulence of the fungus.<sup>[3]</sup> *C. albicans* contains ten different SAP genes, which are differentially expressed at various stages of an infection and are thought to play distinct roles in the infection process.<sup>[4,5]</sup> The SAP2 isoenzyme is the major secretory aspartic protease expressed during in vitro cultivation of *C. albicans* and is required for growth of the fungus on proteins as the sole nitrogen source and for full virulence. SAP2 is also the best-studied protease of *C. albicans* and was the first studied by X-ray crystallography.<sup>[5,6]</sup> Several reversible transition-state-mimetic SAP inhibitors<sup>[7–9]</sup> such as A-70450<sup>[10,11]</sup> (Figure 1 and Figure 9 below) have been developed on the basis of known renin, pepsin, and cathepsin D inhibitors.<sup>[12,13]</sup>

Alternatively, a few reports describe irreversible inhibitors of aspartic proteases based on epoxides. Examples include EPNP (1,2-epoxy-3-(*p*-nitrophenoxy)propane), which is a well known unspecific irreversible inhibitor of aspartic proteases,<sup>[14–16]</sup> and *cis*-configured epoxides known to inhibit HIV-1 protease (Figure 2),<sup>[17–22]</sup> SIV protease,<sup>[23]</sup> and  $\gamma$ -secretase known to be involved in Alzheimer's disease.<sup>[24]</sup> The *cis*-configuration is considered necessary for steric reasons (Figure 3).

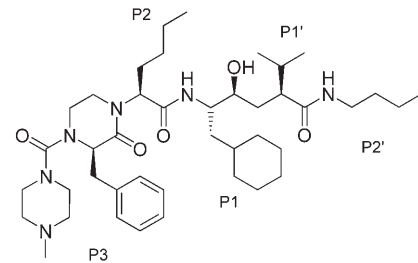


Figure 1. Peptidomimetic inhibitor A-70450 of *Candida* spp. SAP enzymes; the subunits of the inhibitor (P3–P2') are indicated.<sup>[5,10]</sup>

Inhibition is thought to take place by alkylation of one of the active site Asp residues, with the other Asp residue activating the epoxide by protonation prior to or during the ring-

[a] Dr. B. Degel, S. Rohrer, Dr. J. Scheiber, E. Martina, C. Büchold, Prof. Dr. K. Baumann, Prof. Dr. T. Schirmeister  
Institute of Pharmacy and Food Chemistry, University of Würzburg  
Am Hubland, 97074 Würzburg (Germany)  
Fax: (+49) 931-888-5494  
E-mail: schirmei@pzlc.uni-wuerzburg.de

[b] Dr. P. Staib, Prof. Dr. J. Morschhäuser  
Institute for Molecular Infection Biology, University of Würzburg  
Röntgenring 11, 97070 Würzburg (Germany)

[c] S. Rohrer, Prof. Dr. K. Baumann  
Institute for Pharmaceutical Chemistry  
Technical University Carolo-Wilhelmina at Brunswick  
Beethovenstrasse 55, 38106 Braunschweig (Germany)

[d] Dr. P. Staib  
Centre Hospitalier Universitaire Vaudois (CHUV)  
Service de Dermatologie, Av. de Beaumont 29, 1011 Lausanne  
(Switzerland)

Supporting information for this article is available on the WWW under <http://www.chemmedchem.org> or from the author.

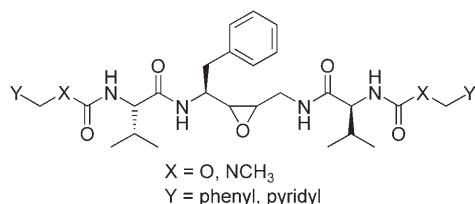


**Figure 2.** Structures of irreversible *cis*-epoxide-based HIV-1 protease inhibitors ( $X = O$ ,  $Y = \text{phenyl}$ ;  $K_i = 0.1 \text{ nM}$ ;  $k_i = 0.015 \text{ min}^{-1}$ ,  $k_i/K_i = 1.5 \times 10^8 \text{ M}^{-1} \text{ min}^{-1}$ ).<sup>[21]</sup>

opening reaction (Figure 3).<sup>[21]</sup> Herein we report our efforts on the design of new inhibitors of *C. albicans* SAP2 based on three-membered heterocycles (epoxides and aziridines). As an initial step we decided to concentrate on variation of the electrophilic moiety that is thought to undergo the covalent reaction with one of the active site Asp residues. The first synthesized compound series includes *cis*-configured epoxide building

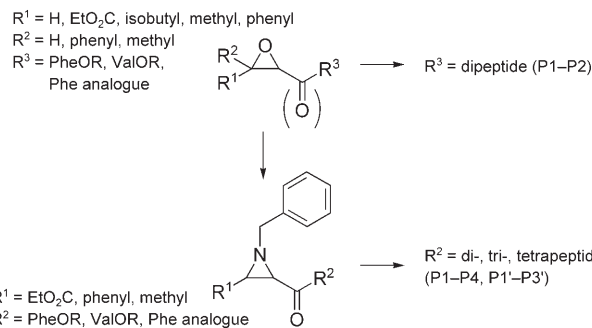


**Figure 4.** Strategy of design of novel *cis*-epoxide- and *cis*-aziridine-based SAP2 inhibitors.

termine if the compounds inhibit *C. albicans* growth due to SAP2 inhibition or due to nonspecific cytotoxic effects. Finally, we performed docking studies to examine possible binding modes.

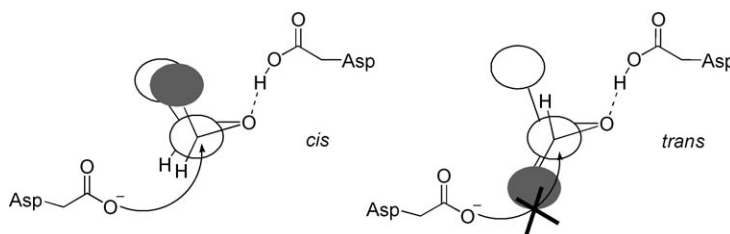


**Figure 3.** Proposed mechanism of inhibition of the HIV-1 aspartic protease by *cis*-configured epoxides.<sup>[23]</sup>

ing blocks containing Phe, Val, or a Phe-analogous moiety (Figure 4). The amino acids Phe and Val were chosen according to the known substrate specificity of SAP2, which prefers hydrophobic amino acids in the P1 and P1' positions. Epoxide building blocks with none (**5a**), one (**4a**, **6a+b**, **6c+d**), or two (**3a+b**, **7a+b**) electron-withdrawing substituents ( $C(=O)NH-R$ ) at the ring carbon atoms were included.

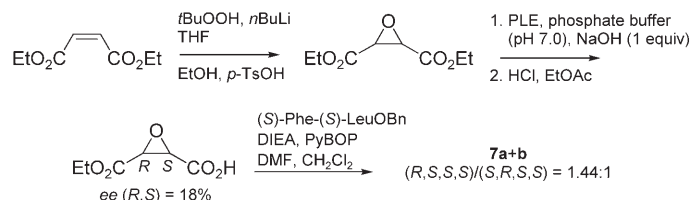
In a second approach we replaced the *cis*-configured epoxide ring by an aziridine (Figure 4), which can also undergo ring-opening reactions with nucleophiles and can be substituted additionally at the aziridine nitrogen atom. Thus, this building block offers broader structural variability. Inhibitors with an *N*-benzyl group and various substituents at C3 of the aziridine ring were included. In a subsequent step we extended the peptide sequence attached to C2 of the three-membered rings to di- and tripeptides according to the prime and non-prime substrate specificity of SAP2 (P1-P4: Phe-Leu-Ala-Pro; P1'-P3': Phe-Ala-Leu). The compounds were tested against SAP2 using a new FRET-pair-labeled substrate. The intra-class selectivity was investigated using the aspartic proteases pepsin and plasminogen II. Because aziridines and epoxides are also suitable as cysteine protease inhibitors,<sup>[25]</sup> the inter-class selectivity was investigated using the cysteine proteases cathepsin B and cathepsin L. Inhibition of *C. albicans* growth was tested in SAP2-dependent and SAP2-independent assays. This was done to de-

## Results and Discussion

### Syntheses of inhibitors

The syntheses of the following compounds were published previously: **1a-d**, **2**, **3a+b**, **5a**, **8a+b**, **8a**, **10d1**, **10d2**, **11a+b**.<sup>[26]</sup> The synthetic pathways of the yet unreported compounds **4**, **6**, **7**, **9**, and **12-17** are briefly described below.

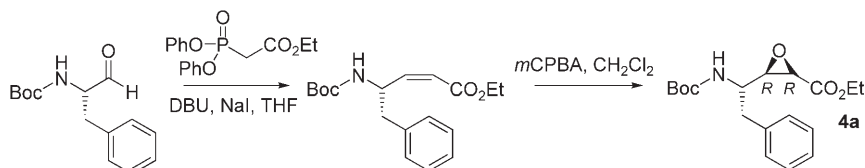
The oxirane-2,3-dicarboxylate derivatives **7a+b** (Scheme 1) were synthesized starting from diethyl maleate through Weitz-Schäffer epoxidation<sup>[27]</sup> and subsequent hydrolysis with pig liver esterase (PLE),



**Scheme 1.** Synthesis of oxirane-2,3-dicarboxylate derivatives **7a+b**.

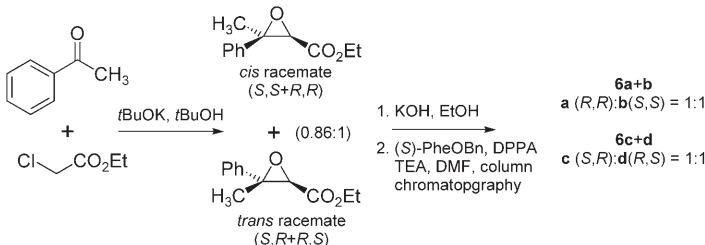
leading to slightly preferred hydrolysis of the ester group at the *S*-configured ring carbon.<sup>[28]</sup> Peptide coupling with PyBOP (1-benzotriazolyl oxytris(pyrrolidino)phosphonium hexafluorophosphate) yielded compounds **7a+b**.

The epoxide-based inhibitor **4a** was synthesized starting from Boc-(S)-phenylalaninal, obtained by DIBAH reduction of Boc-(S)-PheOMe, subsequent Horner-Wadsworth-Emmons olefination<sup>[29]</sup> with ethyl(diphenylphosphono)acetate,<sup>[30]</sup> and finally epoxidation of the obtained *Z*-configured olefin with *m*CPBA (Scheme 2). Due to the *S* configuration of the Phe residue, only the *syn*-configured epoxide (*syn* according to the relative positions of the epoxide oxygen and the nitrogen atom of the Boc-protected amino acid) is obtained.<sup>[31]</sup>



Scheme 2. Synthesis of the epoxide-based inhibitor 4a.

The 2-methyl-2-phenyl-substituted epoxides **6a+b** and **6c+d** were synthesized by glycide ester synthesis,<sup>[32]</sup> hydrolysis, and subsequent DPPA-mediated peptide coupling



Scheme 3. Synthesis of 2-methyl-2-phenyl-substituted epoxides 6a-d.

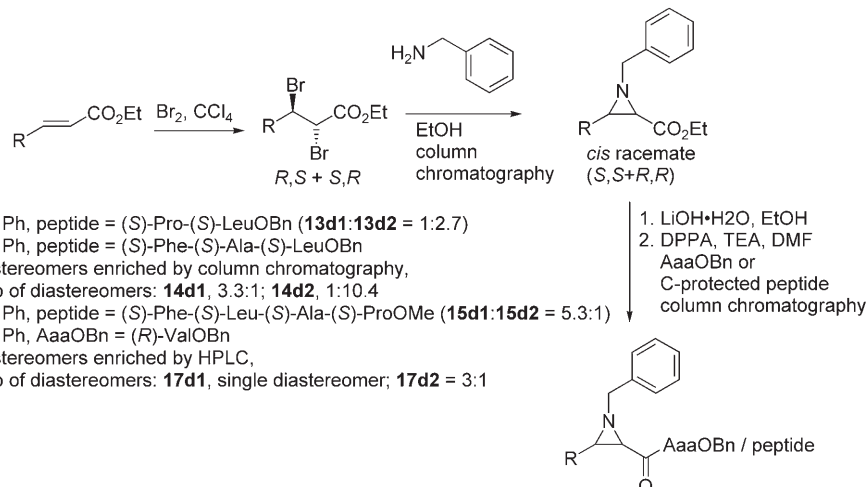
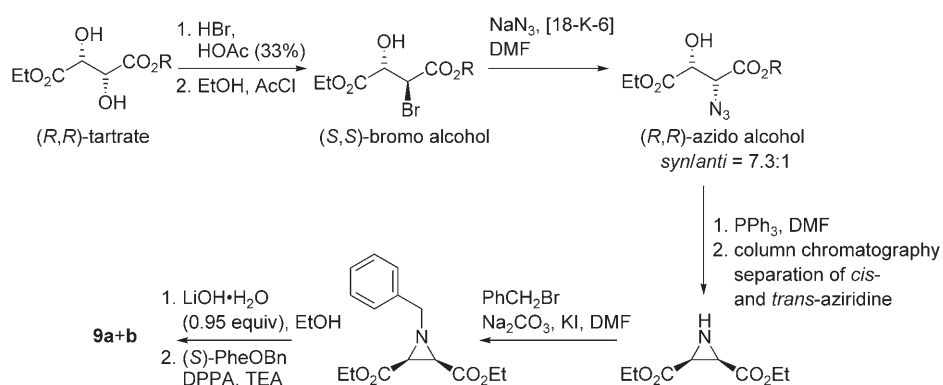
(Scheme 3). The four resulting diastereomers were separated by column chromatography to yield the *cis*-configured diastereomers **6a+b** and the *trans*-configured diastereomers **6c+d**.

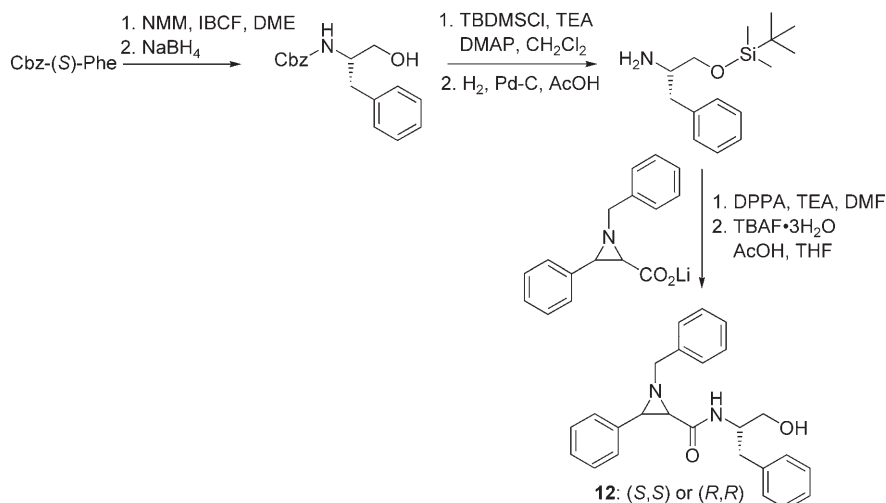
The *N*-benzylated aziridine-2-carboxylic acid derived inhibitors **13**, **14**, **15**, and **17** were obtained by Cromwell synthesis<sup>[33]</sup> starting with cinnamic acid ester, bromination, and ring closure with benzylamine (Scheme 4). Racemates of the *cis*- and *trans*-aziridine-2-carboxylates (*cis/trans* = 4:1) were separated by column chromatography. Hydrolysis of the *cis*-configured esters and DPPA-mediated peptide coupling yielded the inhibitors as diastereomeric mixtures. In all cases one diastereomer was formed preferentially. In two cases (compounds **14** and **17**) the diastereomers were enriched by column chromatography and preparative HPLC, respectively.

The synthesis of the aziridine-2,3-dicarboxylate-derived inhibitor **9a+b** started from (*R,R*)-tartrate (Scheme 5). The (*S,S*)-

bromo alcohol was obtained by a published two-step procedure.<sup>[34]</sup> From this intermediate the azido alcohol<sup>[35]</sup> was obtained through reaction with sodium azide as a mixture of *syn* (*R,R*) and *anti* (*R,S*) diastereomers (*syn/anti* = 7.3:1). These were subjected to ring closure by Staudinger reaction<sup>[36]</sup> to give the *cis*- and *trans*-aziridine-2,3-dicarboxylates, which were separated by column chromatography. Benzylation of the *cis* isomer with benzyl bromide yielded the *N*-benzylated aziridine-2,3-dicarboxylate, which was hydrolyzed and coupled with (*S*)-PheOBn to give the inhibitor **9a+b** as a diastereomeric mixture.

The (*S*)-phenylalaninol derivative **12** (Scheme 6) was obtained by coupling of the racemic *N*-benzylated 2-phenylaziridine-2-carboxylate (Scheme 4) with TBDMS-protected phenylalaninol<sup>[37]</sup> and subsequent deprotection with TBAF. Only one diastereomer could be detected with unknown absolute configuration at the ring carbons.

Scheme 4. Synthesis of *N*-benzylaziridine-2-carboxy derivatives **13**, **14**, **15**, **17**.Scheme 5. Synthesis of the aziridine-2,3-dicarboxylate-derived inhibitor **9a+b**.



**Scheme 6.** Synthesis of the phenylalaninol derivative **12**.

Finally, the succinic acid derivative **16** (Table 1) was obtained by hydrolysis of diethyl succinate with KOH (1 equiv) and subsequent DPPA-mediated coupling with (S)-PheOBn. All compounds are listed in Table 1.

#### New FRET-based enzyme assay and inhibition of SAP2

On the basis of the known substrate specificity of SAP2<sup>[38–40]</sup> a new FRET-pair-labeled peptide was used as substrate for easily practicable fluorimetric enzyme assays: H<sub>2</sub>N-DabcyL-Arg-Lys-Pro-Ala-Leu-Phe-Phe-Arg-Leu-Glu(EDANS)-Arg-CO<sub>2</sub>H, in which the Phe-Phe<sup>[38]</sup> motif serves as scissile P1–P1' dipeptide sequence. At a temperature of 30 °C and a substrate concentration of 37 μM, the fluorescence increase was found to be linear over a period of 30 min. The *K<sub>M</sub>* value for the substrate was determined to be 28.4 ± 2.8 μM (Figure 5). Mass spectrometry of the substrate incubated with SAP2 showed the main cleavage site to be the Phe-Phe bond as expected ([M+H]<sup>+</sup> *m/z* = 967.13 for the N-terminal peptide and [M+H]<sup>+</sup> *m/z* = 965.17

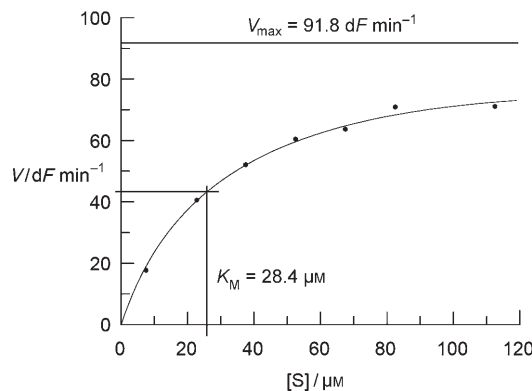


**Figure 5.** Hydrolysis of the FRET-pair-labeled substrate H<sub>2</sub>N-DabcyL-Arg-Lys-Pro-Ala-Leu-Phe-Phe-Arg-Leu-Glu(EDANS)-Arg-CO<sub>2</sub>H by SAP2 from *C. albicans*. For determination of the *K<sub>M</sub>* value, the substrate was used at concentrations between 7.5 and 112.5 μM. Fluorescence increase was measured over a period of 10 min. Values were corrected for the inner filter effect. *K<sub>M</sub>* at 30 °C was determined to be 28.4 ± 2.8 μM.

for the C-terminal peptide), with a very small peak for the C-terminal peptide derived from cleavage between Leu-Phe ([M+Na]<sup>+</sup> *m/z* = 1137.3). With the Phe-Phe dipeptide sequence as the major P1–P1' cleavage site, the substrate is similar to the one used recently for cathepsin D.<sup>[41]</sup>

An initial screening was performed with inhibitor concentrations of 100 μM (Table 2). Compounds showing >50% inhibition in these assays were subjected to detailed studies. First, IC<sub>50</sub> values were determined to allow an initial crude structure–activity relationship

(SAR) analysis. Because for time-dependent inhibitors the second-order rate constants of inhibition (*k<sub>2</sub>*) are the parameters of choice to characterize and compare inhibition potencies, these values were determined by dilution assays which, in a first series, ranged over a period of 30 min.

Analysis of the SARs revealed that the epoxides **1a–d** and **2**, with C3-methyl substituents, are inactive independent of the configuration of the epoxide ring or the amino acid attached. With 12% inhibition at [I] = 100 μM, compound **1c** showed the greatest inhibition within this series. Exchange of the C3-methyl substituent for the electron-withdrawing ethyl ester group (compounds **3a+b**) does not enhance inhibition potency. Enlargement of the peptidic substituent (compounds **7a+b**) also does not have any effect, whereas the epoxide **4a** with a phenylethyl moiety at C2 leads to weak inhibition (25% at [I] = 100 μM). This weak inhibition is lost if the electron-withdrawing ethyl ester substituent is removed (compound **5a**). Only the epoxides **6**, which contain an additional phenyl ring attached to the three-membered ring, show considerable inhibition; the diastereomeric mixture **6c+d**, in which the phenyl ring at C3 is *trans* to the Phe residue at C2, is sixfold more active.

The aziridines **8**, which bear a methyl group at C3 as do the epoxides **1a** and **1c**, but which also contain a benzyl moiety at the aziridine nitrogen, are much more active than the epoxides. Both diastereomers are equipotent. Replacing the methyl group with an ethyl ester (compounds **9a+b**) leads to loss of inhibition, whereas replacement of the methyl group with a phenyl moiety (in **10**) enhances inhibition to a level similar to that of the epoxides. Both enriched diastereomers (**10d1** and **10d2**) are equipotent. Replacing Phe for Val (in **11a+b**) slightly improves inhibition. Compounds **11a+b**, with *k<sub>2</sub>* = 56 756 M<sup>-1</sup> min<sup>-1</sup>, is the most potent inhibitor in the series.

Reducing the Phe benzyl ester to an alcohol (in **12**) leads to complete loss of inhibition. Exchange of PheOBn against the dipeptide Pro-LeuOBn (in **13a+b**) or enlargement of the peptide sequence (compounds **14** and **15a+b**) also decreases inhibitory potency. Because **14d1** is more active than the en-

**Table 1.** Structures of new epoxide- and aziridine-based SAP2 inhibitors.

Compd (Conf. TMR <sup>[a]</sup> )	X	R <sup>4</sup>	R <sup>3</sup>	R <sup>2</sup>	R <sup>1</sup>
<b>1a</b> (R,R)	O	H	H <sub>3</sub> C	C(=O)-(S)-PheOBn	H
<b>1b</b> (R,R)	O	H	H <sub>3</sub> C	C(=O)-(R)-PheOBn	H
<b>1c</b> (S,S)	O	H <sub>3</sub> C	H	H	C(=O)-(S)-PheOBn
<b>1d</b> (S,S)	O	H <sub>3</sub> C	H	H	C(=O)-(R)-PheOBn
<b>2</b> (R,R)	O	H	H <sub>3</sub> C	C(=O)-(S)-ValOBn	H
<b>3a+b</b>	O	H	EtO <sub>2</sub> C	C(=O)-(S)-PheOBn	H
(S,R + R,S; 1.17:1)	O	EtO <sub>2</sub> C	H	H	C(=O)-(S)-PheOBn
<b>4a</b>	O	EtO <sub>2</sub> C	H	H	(S)-CH(Bn)-NH-Boc
<b>5a</b>	O	(H <sub>3</sub> C) <sub>2</sub> HC-H <sub>2</sub> C	H	H	(S)-CH(Bn)-NH-Boc
<b>6a+b</b>	O	H <sub>3</sub> C	phenyl	C(=O)-(S)-PheOBn	H
(R,R + S,S; 1:1)	O	phenyl	H <sub>3</sub> C	H	C(=O)-(S)-PheOBn
<b>6c+d</b>	O	phenyl	H <sub>3</sub> C	C(=O)-(S)-PheOBn	H
(S,R + R,S; 1:1)	O	H <sub>3</sub> C	phenyl	H	C(=O)-(S)-PheOBn
<b>7a+b</b>	O	H	EtO <sub>2</sub> C	C(=O)-(S)-Phe-(S)-LeuOBn	H
(R,S + S,R; 1.44:1)	O	EtO <sub>2</sub> C	H	H	C(=O)-(S)-Phe-(S)-LeuOBn
<b>8a+b</b>	N-Bn	H <sub>3</sub> C	H	H	C(=O)-(S)-PheOBn
(S,S + R,R; 1:1.2)	N-Bn	H	H <sub>3</sub> C	C(=O)-(S)-PheOBn	H
<b>8a</b> (S,S)	N-Bn	H <sub>3</sub> C	H	H	C(=O)-(S)-PheOBn
<b>9a+b</b>	N-Bn	H	EtO <sub>2</sub> C	C(=O)-(S)-PheOBn	H
(R,S + S,R; 1:1.7)	N-Bn	EtO <sub>2</sub> C	H	H	C(=O)-(S)-PheOBn
<b>10d1</b>	N-Bn	H	phenyl	C(=O)-(S)-PheOBn	H
<b>10d2<sup>[b]</sup></b>	N-Bn	phenyl	H	H	C(=O)-(S)-PheOBn
<b>11a+b</b>	N-Bn	H	phenyl	C(=O)-(S)-ValOBn	H
(R,R + S,S; 1:1.4)	N-Bn	phenyl	H	H	C(=O)-(S)-ValOBn
<b>12</b>	N-Bn	H	phenyl	C(=O)-(S)-NH-CH(Bn)-CH <sub>2</sub> OH	H
(R,R or S,S)					
<b>13a+b</b>	N-Bn	H	phenyl	C(=O)-(S)-Pro-(S)-LeuOBn	H
(R,R + S,S; 1:2.7)	N-Bn	phenyl	H	H	C(=O)-(S)-Pro-(S)-LeuOBn
<b>14d1</b>	N-Bn	H	phenyl	C(=O)-(S)-Phe-(S)-Ala-(S)-LeuOBn	H
<b>14d2<sup>[b]</sup></b>	N-Bn	phenyl	H	H	C(=O)-(S)-Phe-(S)-Ala-(S)-LeuOBn
<b>15a+b</b>	N-Bn	H	phenyl	C(=O)-(S)-Phe-(S)-Leu-(S)-Ala-(S)-ProOME	H
(R,R + S,S; 5.3:1)	N-Bn	phenyl	H	H	C(=O)-(S)-Phe-(S)-Leu-(S)-Ala-(S)-ProOME
<b>16<sup>[c]</sup></b>	–	H	EtO <sub>2</sub> C	C(=O)-(S)-PheOBn	H
<b>17d1</b>	N-Bn	H	phenyl	C(=O)-(R)-ValOBn	H
<b>17d2<sup>[b]</sup></b>	N-Bn	phenyl	H	H	C(=O)-(R)-ValOBn

[a] Conf. TMR: absolute configuration of the three-membered ring and ratio of diastereomers in case of diastereomeric mixtures. [b] Column chromatography or preparative HPLC yielded the enriched or pure diastereomers **d1** and **d2** with either R,R or S,S configuration at the TMR in the following ratios of diastereomers: **10d1**, 3.3:1; **10d2**, 1:2.4; **14d1**, 3.3:1; **14d2**, 1:10.4; **17d1**, single diastereomer; **17d2**, 1:3. [c] Succinic acid derivative without TMR.

riched diastereomer **14d2**, inhibition is likely due to one active isomer with the other isomer being inactive. Compound **16**, which does not contain an electrophilic building block, is inactive.

In summary, the results show that a phenyl moiety attached to the three-membered ring is vital for good inhibitory potency. The *N*-benzylated aziridines are more active than related epoxides, which lack the *N*-benzyl moiety (compare **8** vs. **1**, **9** vs. **3**, **10** vs. **6**). It is evident that both the C3-phenyl substituent and the *N*-benzyl moiety are critical for inhibition.

#### Inhibition of *C. albicans* growth

*C. albicans* specifically expresses the SAP2 protease in media containing protein, such as bovine serum albumin (BSA), as the sole nitrogen source.<sup>[42]</sup> SAP2-mediated protein degradation provides nitrogen for cell growth, and *C. albicans* mutants that lack SAP2 are unable to grow in such media.<sup>[43,44]</sup> To deter-

mine the effect of the inhibitors on SAP2-dependent growth of *C. albicans*, strain SC5314 was grown in YCB-BSA medium in the presence of the various inhibitors or solvent (DMSO) only, and the optical density of the cultures was determined after 60 h. To verify that suppression of growth was caused by SAP2 inhibition and not by nonspecific toxic effects of the compounds on the *C. albicans* cells, the same experiments were also performed in YCB-BSA-YE medium, in which SAP2 activity is not required for growth.<sup>[44]</sup>

These assays showed compounds **10d1** and **11a+b** to inhibit SAP2-dependent growth (85 and 88% inhibition, respectively, at an inhibitor concentration of 500  $\mu$ M),<sup>[45]</sup> but not SAP2-independent growth of *C. albicans* (Figure 6). With the exception of compounds **1b** and **1d**, which showed 10–40% growth inhibition in both assays, indicating nonspecific toxicity, all other compounds had no or only weak effects (<10% growth inhibition, data not shown). Because the aziridines **10d1** and **11a+b** also turned out to be the most potent SAP2

**Table 2.** Inhibition of SAP2 isolated from *C. albicans* strain 5314 by epoxide- and aziridine-based inhibitors as determined in fluorimetric enzyme assays.

Compd	Inhibition [%] <sup>[a]</sup>	IC <sub>50</sub> [μM] <sup>[b]</sup>	k <sub>2</sub> [M <sup>-1</sup> min <sup>-1</sup> ] <sup>[c]</sup>
3a+b	0	nd	nd
4a	25±2	nd	nd
5a	14±1.5	nd	nd
6a+b	88±5	40±7	1610±230
6c+d	100	30±4	9890±760
7a+b	0	nd	nd
8a+b	100	58±5	14030±3520
8a	100	22±2	15180±2070
9a+b	17±2	nd	nd
10d1 <sup>[d]</sup>	100	12±3	47955±529
11a+b	100	11±1	56756±1150
13a+b	90±4	55±3	3220±425
14d1 <sup>[d]</sup>	43±4	nd	nd
17d1+d2	100	nd	97440±19970
17d1 <sup>[e]</sup>	100	11±2	96923±4323
17d2	100	7.8±2.5	121674±5088
EPNP	67±3	nd	1083±44
Pepstatin A	100	0.042±0.006 <sup>[f]</sup>	nd

[a] Inhibition of SAP2 at an inhibitor concentration of 100 μM; values represent the mean of two independent assays; all other compounds listed in Table 1 showed no or only weak (<10%) inhibition at [I]=100 μM. [b] IC<sub>50</sub> values determined after 30 min; inhibitors were used at concentrations between 1 and 100 μM; values represent the mean of at least two independent assays. [c] Determined by dilution assays after incubation times of 5, 10, 15, 20, 25, and 30 min; inhibitors were used at concentrations between 1 and 100 μM; because k<sub>obs</sub> vs. [I] plots were restricted to the linear range owing to low inhibitor solubility, the individual inhibition constants k<sub>i</sub> and K<sub>i</sub> could not be determined (except for inhibitor 17d1), and k<sub>2</sub> values were obtained by  $k_2 \approx k_{obs} [I]^{-1} (1 + [S] K_m^{-1})$ ; values represent the mean of at least two independent assays. [d] The enriched diastereomer 10d2 showed equipotent inhibition, indicating no difference in inhibitory activity between the two diastereomers; the enriched diastereomer 14d2 showed no inhibition at 100 μM, indicating that the weak inhibition by 14d1 is due to only one active diastereomer; nd=not determined. [e] k<sub>i</sub>=0.61±0.099 min<sup>-1</sup>; K<sub>i</sub>=6.3±2.3 μM. [f] K<sub>i</sub>=0.0183±0.0026 μM; the inhibitor was used at concentrations between 1 nM and 1 μM; published values: IC<sub>50</sub>=0.027 μM,<sup>[63]</sup> and K<sub>i</sub>=0.006 μM,<sup>[64]</sup> 0.0029 μM,<sup>[63]</sup> and 0.017 μM.<sup>[38]</sup>

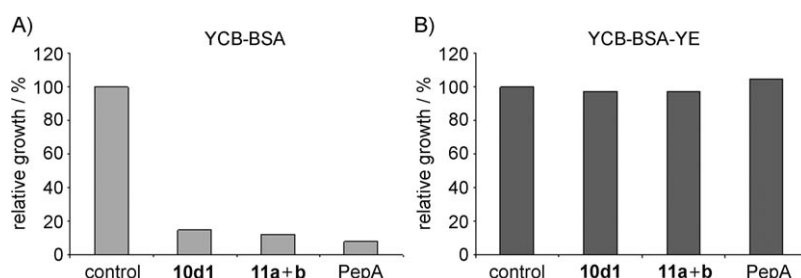


**Figure 6.** A) Inhibition of SAP2-dependent growth of *C. albicans* in YCB-BSA medium by the indicated protease inhibitors. B) SAP2-independent growth in YCB-BSA-YE was not inhibited. The concentration of inhibitors 10d1 and 11a+b in the growth medium was 500 μM; pepstatin A (PepA) was used at 7.3 μM. The strains were grown for 60 h, and the optical densities of the cultures grown in the absence of inhibitors (control, 0.5% DMSO) were set as 100%.

inhibitors in the fluorimetric enzyme assay, these results correlate very well. These compounds do not exhibit nonspecific cytotoxicity at concentrations up to 500 μM. Compound 11a+b was also tested for cytotoxicity using human macrophages.<sup>[26]</sup>

At concentrations up to 100 μM no effects were detected, further proving the low cytotoxicity of the inhibitor.

### Time-dependent inhibition in fluorimetric enzyme assays

In a second series with the most active aziridine-based inhibitors 11 and 17, the incubation times of enzyme and inhibitors prior to substrate addition were extended to 65 min. These assays showed an exponential decrease in enzyme activity over the course of 30–35 min followed by partial recovery, reaching an activity plateau after 50–65 min (Figure 7).<sup>[65]</sup>

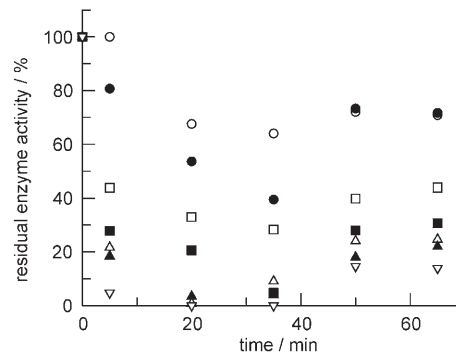
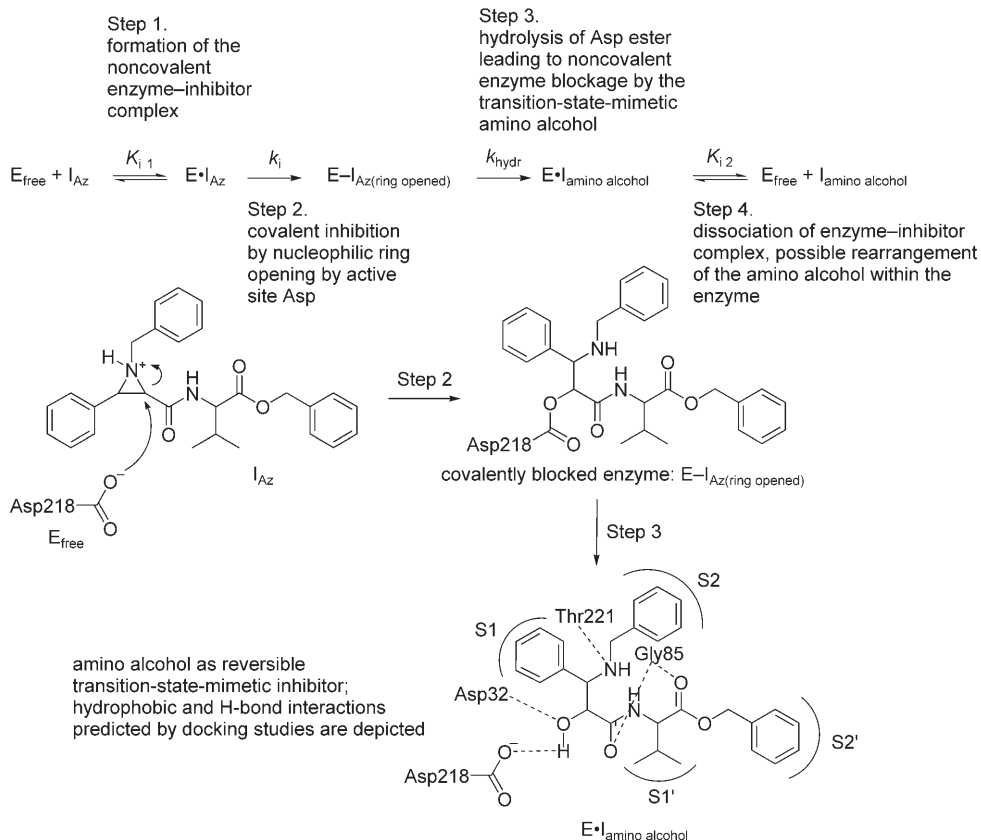


**Figure 7.** Time-dependent inhibition of SAP2 by aziridine 17d1. Enzyme and inhibitor (at the following concentrations: ○ 10, ● 20, □ 40, ■ 50, ▲ 80, ▽ 100 μM) were co-incubated, and aliquots were taken at the indicated time points. The aliquots were diluted with buffer, and the residual enzyme activity was measured by adding substrate. After an exponential decay of the enzyme activity over a period of 30–35 min, the enzyme activity recovered to a certain degree, reaching a plateau after ~50–65 min.

This led us to the hypothesis that the product of the reaction between the enzyme and inhibitor, which represents an aspartic acid ester, might be hydrolyzed under the acidic assay conditions. This would lead to the free enzyme and an amino alcohol which could act as a reversible transition-state-mimetic inhibitor (Scheme 7). To verify this hypothesis, we incubated the enzyme with inhibitor 17 for a period of 65 min under the assay conditions and performed LC-MS studies of the reaction mixture. This assay indeed showed the appearance of a product peak (see Supporting Information) with a molecular weight corresponding to the expected amino alcohol ([M+H]<sup>+</sup> m/z=461.3) proving the pseudo-reversible inhibition of SAP2 by the aziridine-based inhibitors. Ring opening was not observed under the assay conditions in the absence of enzyme, as confirmed by NMR (see Supporting Information) and LC-MS studies. In contrast to other transition-state-mimetic inhibitors based on hydroxy groups (such as pepstatin) the



**Scheme 7.** Model for the pseudo-irreversible dual-mode inhibition of SAP2 by aziridine-based inhibitors. According to the docking studies (see below), Asp 218 is the deprotonated active site Asp residue that attacks the aziridine ring at C2.

inhibitors responsible for the reversible inhibition of SAP2 after longer incubation times are produced within the enzyme itself. According to the classification of enzyme inhibitors<sup>[46]</sup> this inhibition mechanism is similar to “alternate substrate inhibition”, which is normally represented by the reaction:



However, the covalent step leading to the covalently blocked enzyme  $E \cdot I$  is reversible in the case of true alternate substrate inhibitors, whereas in the case of the aziridine-based inhibitors, the covalent step—the ring opening—is irreversible. Furthermore, in the case of alternate substrate inhibitors, the enzyme is not reversibly inhibited by the processed product  $P$  of the inhibitor.

In summary, the dual inhibition mechanism in Scheme 7 can be postulated: This inhibition mechanism has not been described for the previously published epoxide-based inhibitors of other aspartic proteases (such as HIV-1 protease). In our case, the more acidic conditions of the assay medium used for SAP2 might be the reason for the hydrolysis of the intermediate formed Asp ester, because assays at pH 7.0 showed no recovery of the enzyme after 65 min incubation time of enzyme and inhibitor.

### pH-dependent inhibition

SAP2 exhibits its maximum activity at pH values between 3.5 and 3.8.<sup>[8,38]</sup> During *Candida* infections, the fungus produces acidic micro-niches around cells that promote the activity of the SAPs.<sup>[4]</sup> In contrast to epoxide-based inhibitors, the heteroatom of the three-membered ring, the aziridine nitrogen, represents a basic center of the inhibitor. Former quantum chemical calculations<sup>[47]</sup> and experiments<sup>[48]</sup> with aziridines as inhibitors of cysteine proteases have shown that in acidic media the inhibition potency is strongly enhanced, as both the thermodynamics and kinetics of the ring-opening reaction are highly improved. Thus, aziridine-based protease inhibitors represent a class of prodrugs that are activated in acidic media. To evaluate the pH-dependence of inhibition by aziridine-based inhibitors, we measured the residual enzyme activity in comparison with a control at an inhibitor concentration of

50  $\mu\text{M}$  after an incubation time of 5 min (Figure 8).

As expected, the inhibition potency is highest at pH 3.2, where the aziridine nitrogen atom is protonated. This also means that in contrast to the mechanism postulated for *cis*-configured epoxides (Figure 3), the second (protonated) active site aspartic acid residue is not necessary as proton donor.

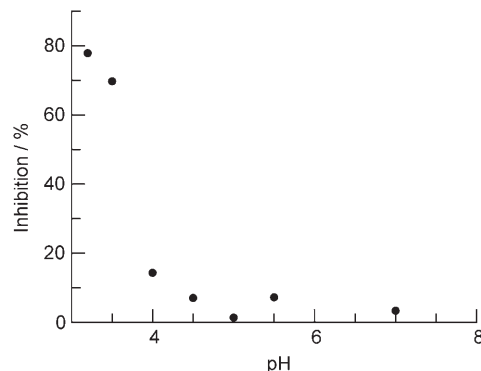


**Figure 8.** pH-dependent inhibition of SAP2 by aziridine 17 at 50  $\mu\text{M}$ .

## Molecular modeling

Docking studies were performed with the X-ray structure of SAP2 (PDB: 1EAG)<sup>[5,6]</sup> and the most active aziridines **10** and **11** using Schrödinger Glide.<sup>[49]</sup> Both diastereomers were docked for each inhibitor, and the pyramidal inversion of the aziridine nitrogen atom was also taken into account. A two-step approach was taken for docking in order to account for the covalent nature of the inhibition mechanism. In an initial step, the ligands were docked in their intact (ring-closed) structures. This simulates the positioning of the ligand in the binding pocket, which is a prerequisite for the formation of the covalent bond. Positioning is dominated by noncovalent interactions that can be readily modeled with the Glide docking software. In the second step, which accounted for the subsequent hydrolysis reaction within the protein, the resulting amino alcohol of each ligand was docked again (see results below).

The scores obtained for all docking solutions were found to be very similar. As a consequence, it was not possible to determine the most likely binding modes by docking score alone. Therefore the 40 best-scoring docking poses resulting from the docking of each ring-closed ligand were visually inspected for enzyme–ligand interactions described by Cutfield et al.<sup>[5]</sup> and Abad-Zapatero et al.<sup>[6]</sup> as crucial for the inhibition of SAP2 by A-70450. The most important of these interactions are: 1) hydrogen bonds to the side chain oxygen atoms of both active site aspartates (Asp 32 and Asp 218), 2) a double hydrogen bond to the backbone nitrogen of Gly 85, 3) a hydrogen bond to a well-ordered water molecule between S2 and S3, and 4) hydrophobic interactions in the S1, S2, S1', and S2' pockets of the protein (Figure 9).

The aziridines **10** and **11** are considerably smaller than the co-crystallized ligand A-70450 and therefore mainly address the S1, S2, S1', and S2' pockets (Figure 10). They do not form

the hydrogen bond to the conserved water molecule; however, the important double hydrogen bond to Gly 85 as well as the hydrogen bond to the active site Asp 218 is formed in both cases. Moreover, hydrophobic contacts are established in all pockets, and there is considerable potential for favorable  $\pi$ – $\pi$  interactions of the *N*-benzyl and 3-phenyl rings with Tyr 84 in S1 and Tyr 225 in S2, respectively (Figure 10). The importance of these hydrophobic interactions is further demonstrated by the fact that compounds lacking phenyl rings in their substituents (such as aziridines **8** and epoxides **6 c,d**) are less active.

From the analysis of the docking poses, no significant difference between the binding modes of the *R,R*- and *S,S*-configured diastereomers was apparent, which is mostly due to the symmetry of the substituents. The *N*-benzyl and 3-phenyl moieties can simply swap places and address the S1 or S2 pocket, respectively (Figure 10).

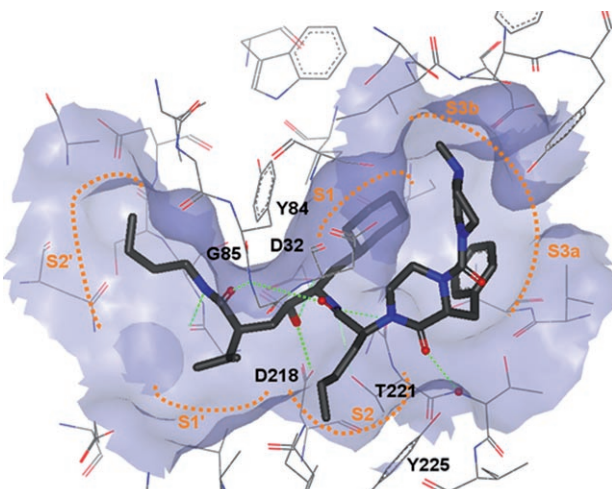
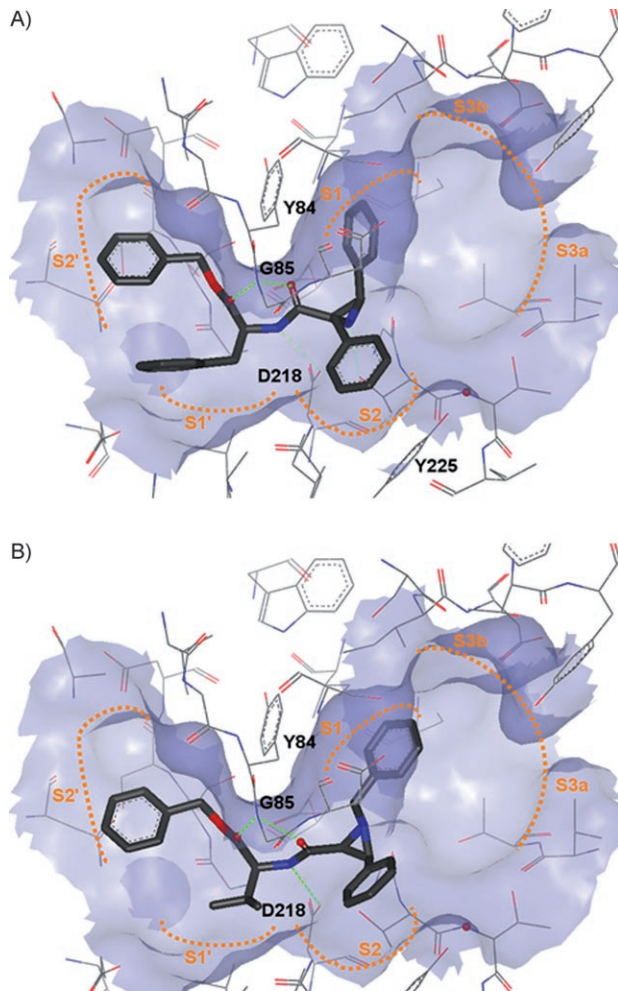


**Figure 9.** The co-crystallized ligand A-70450 bound to SAP2 (PDB: 1EAG). Substrate binding sites are denoted S1–S3 and S1'–S2' in orange. Hydrogen bonds between ligand and enzyme are indicated with green dashes. Most notably, these include bonds to Gly 85, Asp 218, Thr 221, and a well-ordered water molecule. Binding to the S1, S2, S1', and S2' sites is dominated by hydrophobic interactions.

**Figure 10.** A) Predicted binding mode of inhibitor **10** (*R,R*) to the SAP2 binding pocket. Hydrogen bonds to Gly 85 and Asp 218 are formed, and hydrophobic moieties are directed toward the S1, S2, S1', and S2' sites. However, the ring in the (S)-Phe residue of **10** is too bulky to completely fit into the S1' pocket and is exposed to the solvent. The S3 pocket is not addressed. B) The binding mode of inhibitor **11** (*S,S*) is analogous to that of **10**, but the (S)-Val side chain fits better into the S1' pocket. Note the difference between the *R,R* and *S,S* configurations: the *N*-benzyl and 3-phenyl groups swap places between the S1 and S2 sites.

Comparing the binding modes of **10** and **11** shows that the phenyl ring in the (S)-Phe side chain of **10** is too bulky for the S1' pocket and is therefore considerably exposed to the aqueous solvent, explaining the gain in potency by the substitution of Phe by the smaller Val in inhibitor **11**. These findings suggest the potential for optimization of the inhibitors. (R)-Val, for instance, should fit better into the S1' pockets than (S)-Val, establishing closer contacts with less exposure to the aqueous solvent (Figure 11 A).

To verify these predictions, we included a new inhibitor **17**, namely the analogue of inhibitor **11a+b**, which contains (R)-Val instead of (S)-Val. Dilution assays with SAP2 resulted in a  $k_a$  value of  $97\,440\text{ M}^{-1}\text{ min}^{-1}$ , turning the new inhibitor into the most potent within the tested series (Figure 12). The values obtained for the single diastereomers obtained by separation with preparative HPLC do not differ much, indicating that both diastereomers are nearly equipotent, as predicted by the dock-

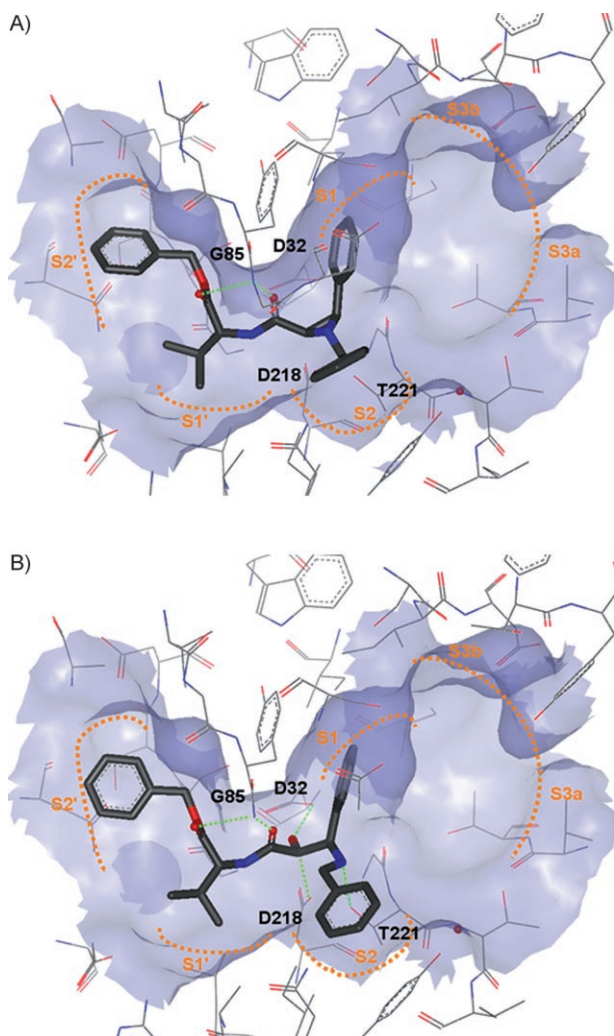


**Figure 11.** Docking results for A) the intact form and B) the ring-opened form of inhibitor **17**. A) The intact form binds tightly to the SAP2 binding pocket with especially tight van der Waals contacts in S2' and S1'. B) The ring-opened form of **17** establishes additional hydrogen bonds to both active site aspartate groups and Thr221. The processed form of **17** can therefore be considered a full-fledged transition-state analogue.

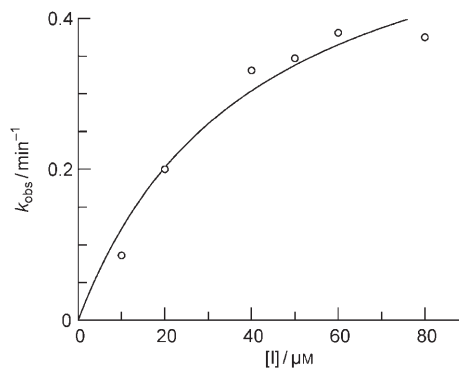


**Figure 12.** SAP2 inhibition by **17d1**:  $k_{\text{obs}}$  vs.  $[I]$ . The following inhibition constants were obtained:  $k_i = 0.61\text{ min}^{-1}$ ,  $K_i = 6.3\text{ }\mu\text{M}$ ,  $k_2 = 96\,923\text{ M}^{-1}\text{ min}^{-1}$ .  $k_{\text{obs}}$  values were obtained by dilution assays at incubation times between 5 and 30 min.

ing studies as well. These experimental results show that the docking studies give a suitable picture of the binding modes of the scrutinized inhibitors.

The docking studies can also be applied to explain why the *trans*-configured epoxides **6c+d** are better inhibitors than **6a+b**: as shown in Figures 10A and 11A, the epoxide **6c+d**, with the phenyl moiety and the Phe ester configured *trans* to each other, could address the S2', S1', and S2 pockets, with the C3 phenyl moiety replacing the *N*-benzyl moiety of the aziridine-based inhibitors. The S1 pocket, then, would not be addressed, explaining the lower inhibition potency relative to the aziridine-based inhibitors.

Docking of the ring-opened and hydrolyzed amino alcohol forms of the inhibitor **17** predicted binding modes analogous to the respective intact ring-closed aziridine forms of the inhibitor (Figure 11). Thus, no considerable rearrangement of the inhibitor in the binding pocket is necessary after the ring opening and subsequent ester hydrolysis. Moreover, the hydroxy group resulting from the hydrolysis reaction forms tight hydrogen bonds to the active site aspartate groups, rendering the processed form of inhibitor **17** a full-fledged transition-state-mimetic inhibitor (Figure 11 B). For inhibitors **10** and **11** the docking of the ring-opened amino alcohols predicted binding modes substantially different from the ring-closed forms (not shown), which means that rearrangements of the reversible inhibitors within the enzyme are necessary.

To assess the potential of inhibitors **10**, **11**, and **17** for cross-reactivity with other aspartate proteases, the structure of SAP2 (PDB: 1EAG) was aligned with the structures of renin (PDB: 1RNE), plasminogen II (1LEE), pepsin (1PSO), and BACE (1W51) using MOE<sup>[50]</sup> (Figure 13). The binding pockets of all five proteins share considerable similarity, especially in the S1, S1', and S2' sites. Because these are the regions mainly addressed by our inhibitors, a certain amount of cross-reactivity cannot be excluded. On the other hand, Figure 13 shows that a substantial degree of dissimilarity is present in the S2 pocket. Regarding future efforts for optimization, the selectivity of the inhibitors might well be enhanced by addressing the S3b pocket, which is completely collapsed in renin and pepsin (Figure 13).

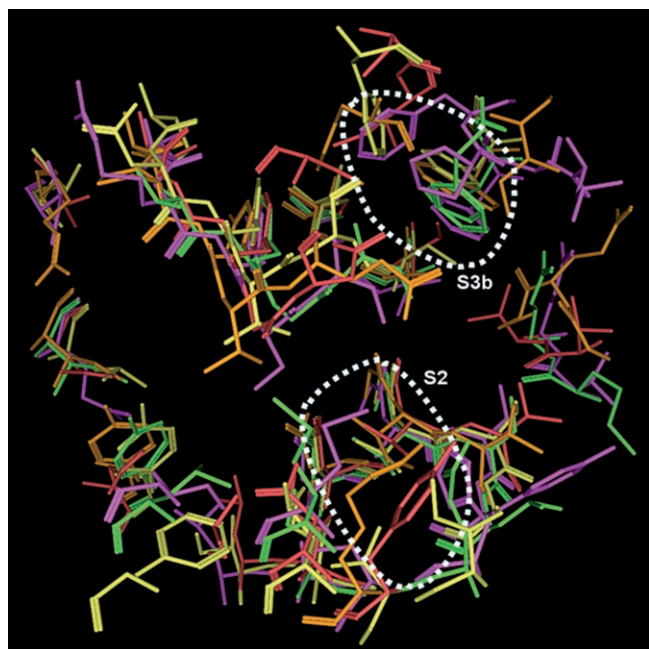


**Figure 13.** Structural alignment of the binding pockets of SAP2 (red), pepsin (green), plasmepsin II (yellow), renin (magenta), and BACE (orange). Although the binding pockets are quite similar in many regions, considerable differences can be observed for the S2 and S3b pockets.

### Inhibition of other aspartic proteases

Compounds **10d1**, **11a+b**, and **17d1+d2** were also tested against pepsin and plasmepsin II from *Plasmodium falciparum*; both enzymes also belong to the pepsin family of aspartic proteases. At concentrations of 100  $\mu$ M, only weak inhibition of plasmepsin II (4–26%) and pepsin (15%) was observed. According to the docking studies described above, this might be due to the dissimilarities within the S2 pockets of the respective enzymes.

### Inhibition of cysteine proteases

The compounds that are active against SAP2 (Table 2) were also tested against the cysteine proteases cathepsin B and L, which belong to the papain-like enzymes (clan CA, family C1).<sup>[51]</sup> At inhibitor concentrations of 200  $\mu$ M, none of the compounds exhibited a percentage inhibition greater than 25%, with compound **8a+b** being the most active against cathepsin L (25% inhibition at 200  $\mu$ M, no inhibition of cathepsin B). This result was expected, as it is known that the three-membered heterocycle needs to be in the *trans* configuration for the inhibition of cysteine proteases of clan CA.<sup>[25]</sup> This is also in agreement with previously published assays that showed the compounds to be only weakly active against viral cysteine proteases (**8a+b**: 34% inhibition at  $[I] = 100 \mu\text{M}$ , **10a+b**: 30%, **1c**: 28%).<sup>[26]</sup>

### Conclusions

The aspartic acid protease SAP2 is the major secretory protease expressed during *in vitro* cultivation of *C. albicans*. Because SAP2 is required for growth of the fungus on a protein food source and for full virulence, this enzyme is considered to be a new potential target for antimycotic drugs with a novel mode of action. A new approach of inhibitor design was pursued: according to *cis*-configured epoxides known to irreversibly inhibit HIV-1 protease by alkylation of one active site Asp residue, this three-membered electrophilic heterocycle was taken as a building block for new inhibitors. Because SAP2 prefers hydrophobic amino acids in the P1 and P1' positions, the epoxide was derivatized with the benzyl esters of the amino acids Phe and Val. To allow facile and accurate determination of inhibition constants, a fluorimetric protease assay using the novel FRET-pair-labeled substrate  $\text{H}_2\text{N-Dabcyl-Arg-Lys-Pro-Ala-Leu-Phe-}||\text{-Phe-Arg-Leu-Glu(EDANS)-Arg-CO}_2\text{H}$  ( $K_M = 28.5 \mu\text{M}$ ) was developed. Initial screening assays showed epoxides with an additional phenyl moiety attached to the ring to be the most active. As the electrophilic aziridine ring allows additional substitution at its nitrogen atom, the aziridine building block was used as novel electrophilic moiety. Thus, a series of *N*-benzyl-substituted aziridines was synthesized and tested. Compounds with a phenyl ring attached to C3 of the aziridine ring and with a Phe or Val ester at C2 (compounds **10** and **11**) turned out to be the most potent inhibitors ( $k_2 \approx 48\,000\text{--}57\,000 \text{ M}^{-1} \text{ min}^{-1}$ ) in a first test series with incubation times up to 30 min. In a second test series using prolonged incubation times, these inhibitors were found to be pseudo-irreversible, exhibiting a dual inhibition mode. The esterified enzyme formed during the aziridine ring opening is hydrolyzed, thus yielding recovered enzyme and transition-state-mimetic amino alcohols that reversibly inhibit the enzyme with  $K_{i(2)}$  values in the low micromolar range.

At concentrations of 100  $\mu\text{M}$ , only weak inhibition of the aspartic proteases pepsin and plasmepsin II was observed. Because aziridine- and epoxide-based inhibitors are also known to inactivate cysteine proteases, the compounds were also tested against cathepsins B and L, and were found to be inactive because of the different stereochemical requirements.

Aziridines **10** and **11** (or rather the respective amino alcohols produced during the inhibition) also inhibit the growth of *C. albicans* in SAP2-dependent *in vitro* assays while being inactive in SAP2-independent assays, proving their low cytotoxicity. The low cytotoxicity was also proven by studies with human macrophages. In addition, modeling studies predict binding modes dominated by hydrophobic interactions with the S1, S2', and S1' pockets of the enzyme, whereas no contacts are made to the S3 pockets. In a subsequent study, a new inhibitor (compound **17**) containing (R)-Val instead of (S)-Val, which—according to the docking studies—should fit better into the S1' pocket, was included and was shown to be more potent than its diastereomeric counterpart, **11**. Docking studies with the processed inhibitor forms, the amino alcohols, predict additional hydrogen bonds to both active site Asp residues. Thus, these can be considered full-fledged transition-state-mimetic

inhibitors. According to the docking studies, the affinity of these inhibitors should be improved by extending the inhibitor structures to the S3 pockets as is the case for A-70450, which exhibits nanomolar affinity.

In conclusion, we showed that *cis*-configured aziridines derivatized with hydrophobic moieties can serve as building blocks for pseudo-irreversible SAP2 inhibitors that show a novel dual-mode mechanism of inhibition. The compounds also display antifungal activity, which is due to the inhibition of SAP2. These compounds are very good starting points for further inhibitor development.

## Experimental Section

### Enzyme assays

The fluorimetric enzyme assays with SAP2 were performed on a Cary Eclipse fluorescence spectrophotometer (Varian, Darmstadt, Germany) using a microplate reader ( $\lambda_{\text{ex}}=355$  nm,  $\lambda_{\text{em}}=540$  nm) using 96-well microplates (Nunc GmbH, Wiesbaden, Germany). The FRET-pair-labeled substrates were products from JPT Peptide Technologies GmbH, Berlin, Germany, or from GenScript Corporation, NJ, USA. SAP2 was obtained as solution from the supernatant of a *C. albicans* culture (see below). This solution was diluted with citrate buffer in such a way that 10  $\mu\text{L}$  dilution (in a total assay volume of 200  $\mu\text{L}$ ) gave a linear fluorescence increase of  $\Delta F \text{min}^{-1} \approx 20$  over a period of 20 min. A citrate buffer (50 mM, pH 3.2) containing 50 mM NaCl was used as buffer. Substrates and inhibitors were dissolved in DMSO (5% final concentration). The final substrate concentration for the determination of inhibition constants was 37.5  $\mu\text{M}$ . The assays were performed at 30 °C. The first screening was performed with inhibitors at a concentration of 100  $\mu\text{M}$ . The residual enzyme activity in the presence of 100  $\mu\text{M}$  inhibitor was determined against a control assay in the absence of inhibitor after co-incubation of enzyme and inhibitor for 30 min prior to substrate addition. For the determination of  $\text{IC}_{50}$ ,  $K_i$ , and  $k_2$  values, the inhibitors were used in a final concentration range of 1–100  $\mu\text{M}$  (100 nM to 100  $\mu\text{M}$  for pepstatin A).  $\text{IC}_{50}$  values were determined by co-incubating enzyme and inhibitor for 30 min prior to the addition of substrate. Second-order inhibition rate constants ( $k_2$  values) were determined by dilution assays according to Kitz and Wilson.<sup>[52]</sup> Enzyme and inhibitor in a defined concentration were incubated, and aliquots were taken after 5, 10, 15, 20, 25, and 30 min. The aliquots were diluted with buffer, substrate was added, and the residual enzyme activities  $[\text{E}]_a$  were determined. These were fitted against the incubation times  $t$  using the exponential decay equation

$$[\text{E}]_a = [\text{E}]_0 e^{-k_{\text{obs}} t} + \text{offset} \quad (2)$$

to yield the pseudo-first-order rate constant of inhibition  $k_{\text{obs}}$ . This was repeated for several inhibitor concentrations  $[\text{I}]$  ranging between 1 and 100  $\mu\text{M}$ . Because plots of  $k_{\text{obs}}$  against  $[\text{I}]$  were, in most cases, restricted to the linear range, the individual constants  $k_i$  (first-order inhibition rate constant) and  $K_i$  (dissociation constant of the noncovalent enzyme–inhibitor complex) could not be determined, and  $k_2$  values were calculated using the equation:

$$k_2 \approx k_{\text{obs}} [\text{I}]^{-1} (1 + [\text{S}] K_M^{-1}) \quad (3)$$

For inhibitor **17d1** the individual constants  $k_i$  and  $K_i$  could be calculated using the hyperbolic equation

$$k_{\text{obs}} = k_i [\text{I}] / (K_i^{\text{app}} + [\text{I}]) \quad (4)$$

and correction to zero substrate concentration from:

$$K_i = K_i^{\text{app}} / (1 + [\text{S}] K_M^{-1}) \quad (5)$$

The second-order rate constant was then obtained by  $k_2 = k_i / K_i$ . The  $K_i$  value for inhibition by pepstatin A was obtained by Dixon plots<sup>[53]</sup> using equation

$$[\text{E}]_0 / [\text{E}]_a = 1 + [\text{I}] / K_i^{\text{app}} \quad (6)$$

and correction to zero substrate concentration from:

$$K_i = K_i^{\text{app}} / (1 + [\text{S}] K_M^{-1}) \quad (7)$$

The pH-dependent inhibition by inhibitor **17** was determined in 50 mM citrate buffers adjusted to the appropriate pH values with an inhibitor concentration of 50  $\mu\text{M}$  and an incubation time of 5 min. In all cases, fluorescence increase was measured over a period of 20 min.

The  $K_M$  value ( $28.4 \pm 2.8 \mu\text{M}$ ) to correct  $K_i^{\text{app}}$  and  $k_2$  values was determined using the substrate in concentrations between 7.5 and 112.5  $\mu\text{M}$ . Fluorescence increase was measured over a period of 10 min for each substrate concentration. Values were corrected for inner filter effect according to Ref. [54].

$K_M$ ,  $\text{IC}_{50}$ ,  $k_{\text{obs}}$ ,  $K_i$ , and  $k_2$  values were calculated by nonlinear or linear regression analyses using the program GraFit.<sup>[55]</sup> All values are mean values from at least two independent assays.

Assays with plasminogen II were performed under the same conditions (buffer, substrate, substrate concentration, and temperature) as described for SAP2. Assays with pepsin were performed according to Ref. [56]. Assays with the cysteine proteases cathepsin B and L were performed as described previously.<sup>[57]</sup>

### LC–MS studies: quantitation of the amino alcohol

The LC–MS studies to detect the hydrolysis product, that is, the respective amino alcohol, were performed with inhibitor **17** (diastereomeric mixture). SAP2 and **17** (final concentration 285  $\mu\text{M}$ ) were incubated for 65 min under the standard assay conditions (total volume 700  $\mu\text{L}$ , 50  $\mu\text{L}$  enzyme solution) described above, except that the inhibitor stock solution was prepared with acetonitrile (final concentration in the assay 5%) instead of DMSO. The reaction mixture was then filtered (Millipore filter: 0.2  $\mu\text{m}$ , hydrophobic PTFE membrane) and subjected to LC–MS: HPLC system 1100, Agilent Phenomenex Jupiter 4  $\mu\text{m}$  Proteo 90A RP C<sub>18</sub> column (4.5  $\times$  150 mm), H<sub>2</sub>O/MeCN gradient (40% MeCN containing 0.1% formic acid for 5 min, 40–95% for 25 min, 95% for 15 min), and detection at 215 nm. The peaks at  $t_R = 10.5$  and 10.9 min possessed a mass of  $[M + H]^+$   $m/z = 461.3$  corresponding to the diastereomeric amino alcohols with the molecular formula C<sub>28</sub>H<sub>32</sub>N<sub>2</sub>O<sub>4</sub> ( $M_r = 460.58$ ; see Supporting Information). The assays were repeated in the absence of enzyme with an incubation time of 65 min with inhibitor **17** in the buffer solution pH 3.2. After 65 min only 1.7% amino alcohol could be detected. To quantify the amino alcohol in the presence of SAP2, the assays were repeated as described above, and aliquots were taken after 15, 30, 60, 120, 180, 240, and 300 min and subjected to LC–MS analysis. The amino alcohol/aziridine ratio was determined by integrating the respective peaks ( $t_R$  for aziridines **17**: 25.3 and 25.8 min; see Supporting Information).

## NMR studies

To prove the stability of aziridine **17** (diastereomeric mixture) under the assay conditions, additional  $^1\text{H}$  NMR studies were performed. A buffer prepared with 50 mM deuterated sodium acetate (pH 3.2) and NaOD was used. The inhibitor stock solution (4.5 mM) was prepared with deuterated acetonitrile.  $^1\text{H}$  NMR spectra were recorded after 10, 20, 30, 40, 50, 60, 75, and 90 min, as well as after 5 h. The integrals of the signals for the aziridine ring protons (doubts at  $\delta$ : 3.10, 3.14, 3.68, and 3.73 ppm) were measured. No changes in the NMR spectra were observed (see Supporting Information).

## *C. albicans* assays

A pre-culture of *C. albicans* strain SC5314 was grown overnight in 10 mL SD medium [6.7 g yeast nitrogen base without amino acids (YNB; Bio101, Vista, CA, USA), 20 g glucose per liter]. Subsequently, the cells were diluted 1:100 in 5 mL SAP2-inducing medium YCB-BSA [23.4 g yeast carbon base (Becton Dickinson, Heidelberg, Germany), 4 g BSA per liter, pH 4.0] and grown for 60 h in a rotary shaker at 225 rpm and 30°C. To monitor SAP2-independent growth, YCB-BSA-YE medium [YCB-BSA supplemented with 0.2% yeast extract (Oxoid, Basingstoke, UK)] was used. For growth assays, the optical density of the cultures was measured photometrically at a wavelength of 600 nm. Stock solutions of inhibitors were prepared in DMSO at a concentration of 100 mM and used at a final concentration of 500  $\mu\text{M}$  except for pepstatin A, which was dissolved in  $\text{CH}_3\text{OH}$  (1 mg  $\text{mL}^{-1}$ ) and used at a final concentration of 5  $\mu\text{g mL}^{-1}$  (7.3  $\mu\text{M}$ ).

For enzyme tests, YCB-BSA cultures of strain SC5314 were centrifuged for 5 min at 4000 rpm. The supernatant, containing SAP2, was sterile filtered and used in the protease assays (see above). SDS-PAGE (12% polyacrylamide; Figure 14) showed the filtrate to

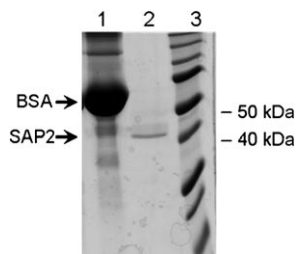


**Figure 14.** Electrophoretic separation of the components of the supernatant of the YCB-BSA culture of strain SC5314 of *C. albicans*: Lane 1) 15  $\mu\text{L}$  supernatant of the strain SC5314, cultivated for 30 h at 30°C in YCB-BSA medium in the presence of pepstatin A, which inhibits *C. albicans* growth by SAP2 inhibition, thus BSA is not degraded. Lane 2) 15  $\mu\text{L}$  supernatant of the strain SC5314, cultivated for 30 h at 30°C in YCB-BSA medium; the supernatant was used for the enzyme assays. Lane 3) standard  $M_r$  values (10 kDa protein ladder, Gibco BRL). Samples were subjected to SDS-PAGE (12% polyacrylamide) and stained with Coomassie blue.

contain only SAP2 as protein. Thus, the enzyme preparation used can be considered pure. Assays with human macrophages (J774.1) were performed as described previously.<sup>[26]</sup>

## Docking

**Preparation of the ligand structures.** All molecules were drawn using Chemaxon MarvinSketch.<sup>[58]</sup> For the ring-closed forms *R,R*

and *S,S* configurations at the aziridine ring were enumerated manually. For the ring-opened forms, all possible positions of the introduced hydroxy group (C2, C3) were enumerated manually as well. After export to MDL SD file format<sup>[59]</sup> implicit hydrogen atoms were added, and ionization states for a pH range of 5±2 were enumerated using Schrödinger LigPrep.<sup>[60]</sup> This pH range includes the conditions of the assay, while allowing for a certain range of local basicity in the protein environment. All aziridine ring nitrogens were predicted to be protonated, and consequently all possible stereoisomers were enumerated for the resulting stereocenter with LigPrep. The same was done for all unspecified chiral centers of the ring-opened forms.

**Preparation of the protein target.** The structure of SAP2 (PDB: 1EAG) was downloaded from the PDB. Except for the well-ordered water molecule described to be involved in ligand binding by Cutfield et al.,<sup>[5]</sup> all waters were removed using MOE.<sup>[50]</sup> After adding hydrogen atoms, the structure was loaded into Schrödinger Maestro.<sup>[61]</sup> H-bond orientation was optimized, and the structure relaxed by a minimization to  $\text{RMSD}=0.30$  using the Schrödinger Protein Preparation wizard.

It is assumed that during proteolysis, one of the active site aspartate residues is present in its protonated form. For SAP2, it is not known which one of the two residues in question (Asp32 or Asp218) is actually protonated. Therefore, all steps described herein, as well as the docking runs, were carried out with both forms: Asp32 or Asp218 protonated. Docking results were similar for both states, but seemed a bit more stable for Asp32 being protonated and Asp218 being deprotonated and thus the residue that attacks the aziridine ring. Moreover, Asp32 is buried deeper than Asp218 and is therefore more likely to be uncharged. Therefore, all figures in this study are based on this form of the protein.

**Docking simulations.** The ligands were docked into the protein active site using Schrödinger Glide<sup>[49]</sup> with default parameters. For the ring-closed forms, a pharmacophore constraint was applied to filter out poses with both aziridine ring carbon atoms more than 3.5 Å away from the deprotonated aspartate residue. No pharmacophore filters were applied for the ring-opened forms. The 40 best scoring poses for each ligand were inspected visually with OpenEye VIDA2,<sup>[62]</sup> which was also used for the generation of all 3D figures for the illustration of the docking results.

## Abbreviations

Bn, benzyl; Boc, *tert*-butyloxycarbonyl; Dabcyll, 4,4-dimethylaminoazobenzene-4'-carboxylic acid; DBU, 1,8-diaza-bicyclo[5.4.0]undec-7-ene; DIBAH, diisobutylaluminum hydride; DIEA, diisopropylethylamine; DME, 1,2-dimethoxyethane; DPPA, diphenylphosphorylazide; EDANS, 5-[(2-aminoethyl)amino]naphthalene-1-sulfonic acid; EPNP, 1,2-epoxy-3-(*p*-nitrophenoxy)propane; FRET, fluorescence resonance energy transfer; IBCF, isobutylchloroformate; *m*CPBA, *m*-chloroperbenzoic acid; NMM, *N*-methylmorpholine; PLE, pig liver esterase; PyBOP, 1-benzo-triazolyloxytris(pyrrolidino)phosphonium hexafluorophosphate; SAP, secreted aspartic acid protease; TBAF, tetrabutylammonium fluoride; TBDMS, *tert*-butyldimethylsilyl; TEA, triethylamine; YCB-BSA, yeast carbon base-bovine serum albumin; YCB-BSA-YE, YCB-BSA supplemented with yeast extract.

## Acknowledgements

Financial support by the DFG (Deutsche Forschungsgemeinschaft) SFB 630 TPA4 (T.S.), TPB2 (J.M. and P.S.), TPC5 (K.B.) is gratefully acknowledged. We thank Prof. Dr. G. Klebe, Institute for Pharmaceutical Chemistry, University of Marburg, for supplying us with plasmeprin II from *P. falciparum*. We also thank Prof. Dr. A. Ponte-Sucre, University of Würzburg, Institute for Molecular Infection Biology, for performing the cytotoxicity tests with macrophages. P.S. is the recipient of a fellowship from the Deutsche Akademie der Naturforscher Leopoldina (Förderkennzeichen BMBF-LPD 9901/8-146).

**Keywords:** aspartic proteases • aziridines • *Candida albicans* • epoxides • inhibitors

- [1] M. Nucci, K. A. Marr, *Clin. Infect. Dis.* **2005**, *41*, 521–526.
- [2] M. D. Richardson, *J. Antimicrob. Chemother.* **2005**, *56*, i5–i11.
- [3] K. Stewart, C. Abad-Zapatero, *Curr. Med. Chem.* **2001**, *8*, 941–948.
- [4] J. R. Naglik, S. J. Challacombe, B. Hube, *Microbiol. Mol. Biol. Rev.* **2003**, *67*, 400–428.
- [5] S. M. Cutfield, E. J. Dodson, B. F. Anderson, P. C. Moody, C. J. Marshall, P. A. Sullivan, J. F. Cutfield, *Structure* **1995**, *3*, 1261–1271.
- [6] C. Abad-Zapatero, R. Goldman, S. W. Muchmore, C. Hutchins, K. Stewart, J. Navaza, C. D. Payne, T. L. Ray, *Protein Sci.* **1996**, *5*, 640–652.
- [7] I. Pichová, L. Pavlicková, J. Dostál, E. Dolejsi, O. Hrušková-Heidingsfeldová, J. Weber, T. Rumí, M. Souček, *Eur. J. Biochem.* **2001**, *268*, 2669–2677.
- [8] D. Backman, U. H. Danielson, *Biochim. Biophys. Acta Proteins Proteomics* **2003**, *1646*, 184–195.
- [9] A. Tossi, F. Benedetti, S. Norbedo, D. Skrbec, F. Berti, D. Romeo, *Bioorg. Med. Chem.* **2003**, *11*, 4719–4727.
- [10] C. Abad-Zapatero, R. Goldman, S. W. Muchmore, C. Hutchins, T. Oie, K. Stewart, S. M. Cutfield, J. F. Cutfield, S. I. Foundling, T. L. Ray, *Adv. Exp. Med. Biol.* **1998**, *436*, 297–313.
- [11] S. K. Pranav Kumar, V. M. Kulkarni, *Bioorg. Med. Chem.* **2002**, *10*, 1153–1170.
- [12] M. C. Bursavich, D. H. Rich, *J. Med. Chem.* **2002**, *45*, 541–558.
- [13] B. M. Dunn, *Chem. Rev.* **2002**, *102*, 4431–4458.
- [14] K. C. S. Chen, J. Tang, *J. Biol. Chem.* **1972**, *247*, 2566–2574.
- [15] R. B. Rose, J. R. Rose, R. Salto, C. S. Craik, R. M. Stroud, *Biochemistry* **1993**, *32*, 12498–12507.
- [16] R. Salto, L. M. Babe, J. Li, J. R. Rose, Z. Yu, A. Burlingame, J. J. De Voss, Z. Sui, P. Ortiz de Montellano, C. S. Craik, *J. Biol. Chem.* **1994**, *269*, 10691–10698.
- [17] C. S. Lee, N. Choy, C. Park, H. Choi, Y. C. Son, S. Kim, J. H. Ok, H. Yoon, S. C. Kim, *Bioorg. Med. Chem. Lett.* **1996**, *6*, 589–594.
- [18] Z. Yu, P. Caldera, F. McPhee, J. J. De Voss, P. R. Jones, A. L. Burlingame, I. D. Kuntz, C. S. Craik, P. R. Ortiz de Montellano, *J. Am. Chem. Soc.* **1996**, *118*, 5846–5856.
- [19] S. Ro, S.-G. Baek, B. Lee, J. H. Ok, *J. Pept. Res.* **1999**, *54*, 242–248.
- [20] A. D. Abell, D. A. Hoult, D. A. Bergman, D. P. Fairlie, *Bioorg. Med. Chem. Lett.* **1997**, *7*, 2853–2856.
- [21] C. Park, J. S. Koh, Y. C. Son, H. Choi, C. S. Lee, N. Choy, K. Y. Moon, W. H. Jung, S. C. Kim, H. Yoon, *Bioorg. Med. Chem. Lett.* **1995**, *5*, 1843–1848.
- [22] S. K. Grant, M. L. Moore, S. A. Fakhouri, T. A. Tomaszek, Jr., T. D. Meek, *Bioorg. Med. Chem. Lett.* **1992**, *2*, 1441–1445.
- [23] P. S. Caldera, Z. Yu, R. M. A. Knegtel, F. McPhee, A. L. Burlingame, C. S. Craik, I. D. Kuntz, P. R. Ortiz de Montellano, *Bioorg. Med. Chem.* **1997**, *5*, 2019–2027.
- [24] S. C. Piper, Z. Amtul, L. Galinanes-Garcia, V. G. Howard, C. Ziani-Cherif, C. McLendon, M. J. Rochette, A. Faug, T. E. Golde, M. P. Murphy, *Biochem. Biophys. Res. Commun.* **2003**, *305*, 529–533.
- [25] J. C. Powers, J. L. Asgian, O. D. Ekici, K. E. James, *Chem. Rev.* **2002**, *102*, 4639–4750.
- [26] R. Vicik, V. Hoerr, M. Glaser, M. Schultheis, E. Hansell, J. H. McKerrow, U. Holzgrabe, C. R. Caffrey, A. Ponte-Sucre, H. Moll, A. Stich, T. Schirmeister, *Bioorg. Med. Chem. Lett.* **2006**, *16*, 2753–2757.
- [27] a) C. Clark, P. Hermans, O. Methcalf, C. Moore, H. C. Taljaard, G. J. Vanvuuren, *Chem. Soc. Chem. Commun.* **1986**, 1378–1380; b) O. Methcalf, C. Moore, H. C. Taljaard, *J. Chem. Soc. Perkin Trans. 1* **1988**, 2663–2674.
- [28] D. Häbich, W. Hartwig, *Tetrahedron Lett.* **1987**, *28*, 781–784.
- [29] a) K. Ando, T. Oishi, M. Hirama, H. Ohno, T. Ibuka, *J. Org. Chem.* **2000**, *65*, 4745–4749; b) P. M. Pihko, T. M. Salo, *Tetrahedron Lett.* **2003**, *44*, 4361–4364.
- [30] K. J. Ando, *J. Org. Chem.* **1997**, *62*, 1934–1939.
- [31] a) A. Jenmalm, W. Berts, Y. L. Li, K. Luthman, I. Croregh, U. Hacksell, *J. Org. Chem.* **1994**, *59*, 1139–1148; b) D. Scholz, A. Billich, B. Charpiot, P. Ettmayer, P. Lehr, B. Rosenwirth, E. Schreiner, H. Gstach, *J. Med. Chem.* **1994**, *37*, 3079–3089.
- [32] a) J. M. Domagala, R. D. Bach, *J. Org. Chem.* **1979**, *44*, 3168–3174; b) K. Kimata, M. Kobayashi, K. Hosoya, T. Araki, N. Tanaka, *J. Am. Chem. Soc.* **1996**, *118*, 759–762.
- [33] a) P. Davoli, A. Forni, I. Moretti, F. Prati, G. Torre, *Tetrahedron* **2001**, *57*, 1801–1812; b) P. Davoli, I. Moretti, F. Prati, H. J. Alper, *J. Org. Chem.* **1999**, *64*, 518–521.
- [34] K. Mori, H. Iwasawa, *Tetrahedron* **1980**, *36*, 87–90.
- [35] F. B. Charvillon, R. Amouroux, *Synth. Commun.* **1997**, *27*, 395–403.
- [36] P. Pöchlauer, E. P. Muller, P. Peringer, *Helv. Chim. Acta* **1984**, *67*, 1238–1247.
- [37] a) M. Rodriguez, M. Llinas, S. Doulut, A. Heitz, J. Martinez, *Tetrahedron Lett.* **1991**, *32*, 923–926; b) M. Ihara, A. Katsumata, F. Setsu, Y. Tokunaga, K. Fukumoto, *J. Org. Chem.* **1996**, *61*, 677–684; c) E. Medina, A. Moyano, M. A. Pericas, A. J. Riera, *J. Org. Chem.* **1998**, *63*, 8574–8578; d) T. Isobe, K. Fukuda, K. Yamaguchi, H. Seki, T. Tokunaga, T. Ishikawa, *J. Org. Chem.* **2000**, *65*, 7779–7785.
- [38] G. Koelsch, J. Tang, J. A. Loy, M. Monod, K. Jackson, S. I. Foundling, X. L. Lin, *Biochim. Biophys. Acta Protein Struct. Mol. Enzymol.* **2000**, *1480*, 117–131.
- [39] M. Fusek, E. A. Smith, M. Monod, B. Dunn, S. I. Foundling, *Biochemistry* **1994**, *33*, 9791–9799.
- [40] D. Skrbec, D. Romeo, *Biochem. Biophys. Res. Commun.* **2002**, *297*, 1350–1353.
- [41] N. Goldfarb, M. T. Lam, A. K. Bose, A. M. Patel, A. J. Duckworth, B. M. Dunn, *Biochemistry* **2005**, *44*, 15725–15733.
- [42] B. Hube, M. Monod, D. A. Schofield, A. J. Brown, N. A. Gow, *Mol. Microbiol.* **1994**, *14*, 87–99.
- [43] B. Hube, D. Sanglard, F. C. Odds, D. Hess, M. Monod, W. Schafer, A. J. Brown, N. A. Gow, *Infect. Immunol.* **1997**, *65*, 3529–3538.
- [44] P. Staib, M. Kretschmar, T. Nichterlein, H. Hof, J. Morschhäuser, *Mol. Microbiol.* **2002**, *44*, 1351–1366.
- [45] This concentration is equipotent to 7.3  $\mu$ M pepstatin A, which has an IC<sub>50</sub> of 0.042  $\mu$ M against SAP2.
- [46] L. J. Copp in *Enzyme Kinetics, a Modern Approach* (Ed.: E. G. Marangoni), Wiley, New York, **2003**, ch. 13, p. 158–173.
- [47] H. Helten, T. Schirmeister, B. Engels, *J. Phys. Chem. A* **2004**, *108*, 7691–7701.
- [48] a) V. Martichonok, C. Plouffe, A. Storer, R. Menard, J. B. Jones, *J. Med. Chem.* **1995**, *38*, 3078–3085; b) T. Schirmeister, M. Peric, *Bioorg. Med. Chem.* **2000**, *8*, 1281–1291.
- [49] Glide, Schrödinger, LLC, New York, NY, USA, **2007**.
- [50] MOE Molecular Operating Environment, Chemical Computing Group, Inc., Montreal, Canada, **2006**.
- [51] A. J. Barrett, N. D. Rawlings, *Biol. Chem.* **2001**, *382*, 727–733.
- [52] R. Kitz, I. B. Wilson, *J. Biol. Chem.* **1962**, *237*, 3245–3249.
- [53] P. J. F. Henderson, *Biochem. J.* **1972**, *127*, 321–333.
- [54] Y. Y. Liu, W. Kati, C. M. Chen, R. Tripathi, A. Molla, W. Kohlbrenner, *Anal. Biochem.* **1999**, *267*, 331–335.
- [55] Graft, Version 5.0.13, Eritracus Software Ltd., London, UK, **2006**.
- [56] K. Inouye, J. Fruton, *Biochemistry* **1967**, *6*, 1765–1777.
- [57] R. Vicik, M. Busemann, C. Gelhaus, N. Stiefl, J. Scheiber, W. Schmitz, F. Schulz, M. Mladenovic, B. Engels, M. Leippe, K. Baumann, T. Schirmeister, *ChemMedChem* **2006**, *1*, 1126–1141.
- [58] Marvin Sketch, ChemAxon Kft., Budapest, Hungary, **2006**.
- [59] CTFile Formats, MDL Information Systems, Inc., San Ramon, CA, USA, **2005**.

[60] LigPrep, Schrödinger, LLC, New York, NY, USA, 2005.

[61] Maestro, Schrödinger, LLC, New York, NY, USA, 2007.

[62] VIDA2, OpenEye Scientific Software, Inc., Santa Fe, NM, USA, 2006.

[63] J. O. Capobianco, C. G. Lerner, R. C. Goldman, *Anal. Biochem.* **1992**, *204*, 96–102.

[64] M. Fusek, E. A. Smith, M. Monod, B. M. Dunn, S. I. Foundling, *Biochemistry* **1994**, *33*, 9791–9799.

[65] Assays with 10 and 20  $\mu$ M inhibitor showed that the percentage of residual enzyme activity remained constant at ~70% over a period of 140 min.

---

Received: May 2, 2007

Revised: October 15, 2007

Published online on November 23, 2007

---